Reduction of Radiation-Induced False Counts in Inspection Systems

Stephen Biellak, Christian Wolters, Anatoly Romanovsky
Surfscan-ADE Division

Abstract – Background radiation is found to be a substantial contributor to false counts in an unpatterned inspection system utilizing CCD sensors. We have measured a background event flux of approximately 1.5 cm^{-2} min^{-1}, consistent with previous literature observations. Given this value, achieving acceptable false count rates requires multiple countermeasures. We outline these strategies and describe a coincident detector measurement system that we believe can reject false counts due to muons.

I. Introduction

False positives are undesirable in inspection applications. For example, in un-patterned or monitor wafer inspection, systems are typically configured to allow for less than one false count per wafer scanned. The tradeoff between false count rate and sensitivity or capture rate in inspection systems is well understood [1].

These false positives can arise from radiation sources, both nearby and distant. Background radiation consists of the decay of trace levels of nearby radioactive isotopes, and high energy cosmic radiation by-products generated in the atmosphere, both directly and via inelastic scattering from materials in close proximity. For example. muons, primarily generated in the upper atmosphere via cosmic rays, have a flux at sea level of approximately 1 cm^{-2} min^{-1} [2]. These and other particles impinge on inspection system detectors and can mimic the signals expected from real sample defects.

In the past, the sensitivity of typical two-dimensional silicon-based detectors to background radiation such as muons and gammas has been studied within the astronomy community [3]. In such applications, even relatively low-level radiation is problematic due to the low readout noise and high sensitivity enabled by modest sampling rates.

At KLA-Tencor, instances of radiation-induced events in CCD sensors have also been previously observed. For example, in RAPID, alpha particle decays from electronic packaging material elements and trace radon gas were detected [4]

However, many two-dimensional CCDs employed in KLA-Tencor systems have heretofore been insensitive to other types of background radiation. This is due in part to an emphasis on total charge capacity, resulting in relatively low charge-to-voltage conversion CCD gain. But now, the planned insertion of these sensors into unpatterned inspection systems has necessarily increased this conversion gain, in order to better detect small objects on an often featureless background, and has thereby made these radiation events an important consideration in such systems.

In this paper, we first present statistics of radiation events detected by our CCDs. We then discuss strategies to reduce the event rate to an acceptable level, in particular a coincident detection method.

II. Experimental Methods and Results

A CCD sensor with a net conversion gain of approximately 45 photoelectrons per DN (gray levels) was characterized. The sensor was operated within a nitrogen-purged ceramic

package cavity sealed by a fused silica window, in order to remove atmospheric radon. Sets of 1e14 or more dark samples (pixels) were collected under various conditions. A representative outlier histogram cataloging all events of total magnitude greater than 14 gray levels (i.e., 630 generated photo-electrons), after correction for camera dark offset, is shown in Figure 1.

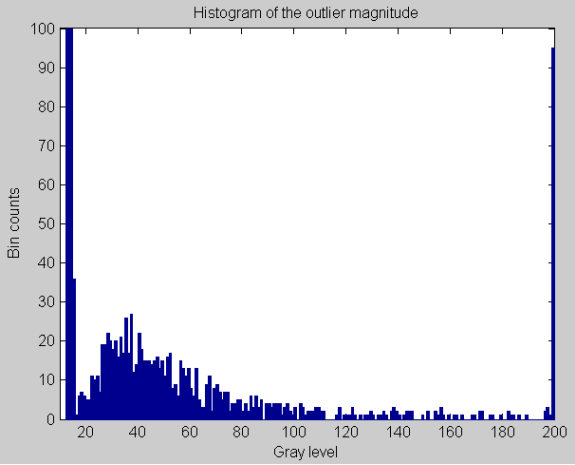

Fig 1: Sensor outlier histogram. One gray level corresponds to 45 photoelectrons. In this data set, 980 events were observed in 690 minutes of data collection, corresponding to 1.04e14 total samples. The histogram is truncated at 200 gray levels and all higher magnitude events are binned at that level.

Virtually all events below 18 grey levels in this histogram are thought to be from the "tail" of the camera readout noise distribution, which is close to Gaussian and has a one-sigma value of approximately 2.17 grey levels after a 2x2 spatial convolution. As many un-patterned inspection use cases have background levels on the order of one gray level per pixel, this sensor dark noise is often the dominant system noise source. Therefore, despite this histogram being obtained in dark conditions, potentially all the events shown in Figure 1 will be registered as false defect counts, unless the detection threshold is increased beyond the ideal value of 18.

The apparent peak in the histogram of approximately 35 gray levels is consistent with the calculated cross section for muons incident on silicon of identical thickness, as described elsewhere [5].

Figure 2 shows the outlier event rate is well described by Poisson statistics. In this case, the mean outliers per minute is 1.42, which corresponds to 1.49 cm^{-2} min^{-1}, given the area of the active region of the sensor.

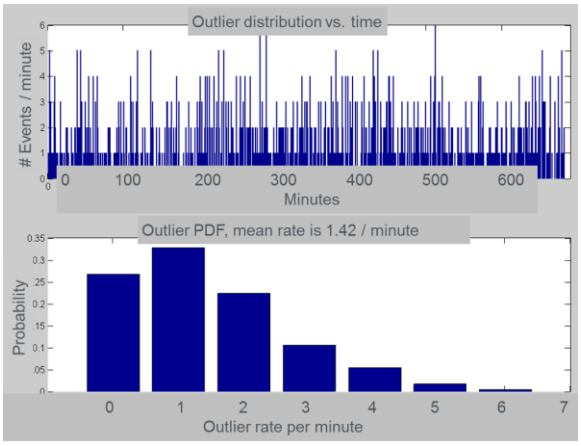

Fig 2: Outlier rate as a function of time and described as a PDF. Sensor was positioned horizontally.

As muons are known to have anistropic flux which peaks from the direction of the zenith, a comparison is made in Table 1 between a sensor positioned vertically and a sensor positioned horizontally. Consistent with expectations, the false rate is reduced for the vertically positioned sensor.

Table 1: Sensor outlier rate versus sensor orientation

Sensor Spatial Orientation	Vertical	Horiontal
Outlier Rate per minute	1.26	1.62

Figure 3 compares the energy distribution of the events in these two cases. Virtually all the excess event counts in the horizontally positioned sensor relative to the vertically positioned sensor are located in the region of the peak observed in Figure 1.

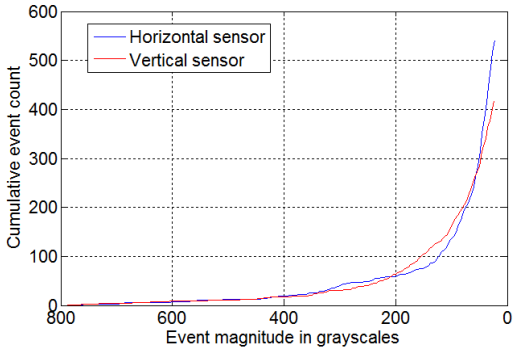

Fig. 3: Cumulative event count vs. event magnitude for horizontal sensor and for vertical sensor. Note the horizontal axis begins with the largest magnitude events.

From these data, we estimate that approximately one half of the observed radiation events are anisotropically incident events, likely muons. The rest are possibly gamma background, from terrestrial sources, as well as "skyshine", which combined have a broad energy distribution and a more isotropic angular distribution [6].

Independently, we characterized individual components of the sensor assembly (heat sink, mounting mechanics, and ceramic package) inside a lead shielded chamber, using both a Gamma detector and a Geiger-Muller tube, and did not observe any additional radiation signature for any component above the reduced background levels.

III. Discussion

Based on these data, we derived an expected false count rate for our inspection system, taking into account the anticipated increase in radiation at higher-elevation customer sites. At 50 wafers per hour (wph), the average event rate for every wafer inspected could exceed the allowable level by a factor of five or more. Therefore, for this new inspection system, radiation counter-measures are necessary.

Many of these countermeasures are straightforward. Sensor pixel size should be minimized to the extent possible while still maintaining other characteristics such as full well, MTF, and speed. As demonstrated in the previous section, vertically positioned sensors confer obvious benefits. Furthermore, High-Z material of sufficient purity should shield as much of the available sensor solid angle as possible, and thereby eliminate most non-muon radiation counts. Table 2 compares the absorption of gamma radiation and of muons in tungsten. An average atmospheric muon at sea level has an energy of 4 GeV and therefore thin shielding of any type of material has little impact. On the other hand, gamma (and lower energy X-ray) radiation can be well controlled.

Table 2: Attenuation of gamma and muon radiation by tungsten. Note different units. Data derived from [7] [8]

Attenuation Coefficient (cm^{-1})		Energy Loss Coefficient ($MeV\ cm^{-1}$)
100 KeV γ	**1 MeV γ**	**4 GeV μ**
64.8	1.08	29 .1

On the data processing side, advantage can be taken of the fact that radiation events are not convolved by the system point spread function. In our un-patterend inspection use case, where the point spread function is undersampled to enable high throughputs, we believe 30% or more of the outliers can be filtered based on initial simulations. With higher sampling resolution, we expect this rejection percentage can be substantially increased.

Also, as our system has multiple sensors configurable to collect various portions and/or polarizations of the scattering hemisphere, some comparison of the individual sensor outputs may be made to reject outliers. While such a multi-channel filter can be highly effective at eliminating radiation, capture rate of certain defect types could be reduced, and therefore it must be characterized for each potential use case.

Coincidence hardware detection is another approach that can eliminate muon events. The concept of a coincidence detector has been previously described [9]. It works as follows: in close proximity to every inspection sensor, a second sensing device is positioned. This coincidence detector will preferably subtend as large a solid angle as possible through which muons traverse and impinge upon the actual system sensor. A relatively low-cost single-pixel device made of a thin plastic scintillator with an end-coupled PMT can be employed. By comparing the arrival time of candidate events on both sensors, "coincident" events can be rejected. One possible implementation of this coincidence detector is shown in Figure 4.

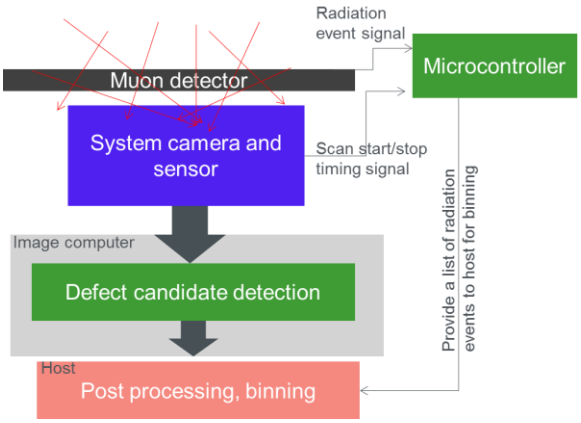

Figure 4: One potential coincidence detection sub-system implementation

It is straightforward to calculate the time resolution of the coincidence detector needed to ensure a minimal number of false coincidences. It can be found that a relatively modest time resolution is needed on the order of tens of microseconds for a 1% false coincident rate, even when the coincidence detector is large and detects many muons not coincident on the system sensor.

Table 3 shows the results from a simplified feasibility demonstration study. In this experiment, two identical Geiger-Muller tubes were placed at varying distances from each other. A consumer-level micro-controller processed the event signals from both tubes. More than 30% of the detected events were coincidences at close range. With 20 cm separation, the number of coincidences dropped to zero in ten minutes, a reasonable result given the detector type .

Table 3: Coincident measurement results from two Geiger counters for a period of ten minutes

Configuration	Detector #1 counts per minute	Detector #2 counts per minute	Conicidence counts per minute
Detectors Adjacent	34.1	35.0	11.3
Detectors Separated by 20 cm	37.8	35.4	0

At the present time, we are in the process of developing full-scale prototype hardware for utilization in conjunction with our actual system sensors, and expect to report on the results soon. We anticipate rejecting up to 80% of the muon events in this fashion, and a higher ratio may be possible, dependent on the solid angle coverage we achieve with the coincident detector.

IV. Conclusion

The use of sensors sensitive to muons and other background radiation has been observed to potentially result in substantial inspection false counts. False count control can be achieved through a multi-step approach including shielding, coincidence observation, and coincident detection.

Acknowledgments

The authors acknowledge Mous Tatarkhavnov, Ximan Jiang, Rohit Patnaik, Howard Chern, Guowu Zheng, Tyler Trytko, Dan Kavaldjiev, Venkat Iyer, and Don Pettibone for supporting this work.

V. Bibliography

1 SEMI Standards, "M50-0310 TEST METHODS FOR DETERMINING CAPTURE RATE AND FALSE COUNT RATE FOR SURFACE SCANNING INSPECTION SYSTEMS BY THE OVERLAY METHOD".

2 "Muons," [Online]. Available: http://cosmic.lbl.gov/SKliewer/Cosmic_Rays/Muons.htm.

3 D. E. Groom, "Cosmic Rays and other nonsense in astronomical CCD imagers," *Experimental Astronomy*, vol. 14, no. 1, pp. 45-55, 2002.

4 V. Iyer, "Fast Localized Report," , RAPID Division, 2008.

5 A. R. Smith et al, "Radiation events in astronomical CCD images," in *Electronic Imaging 2002, International Society for Optics and Photonics*, 2002.

6 A. L. Mitchell et al, "Skyshine contribution to gamma ray background between 0 and 4 MeV," Pacific Northwest Laboratory, 2009.

7 D. R. Nelson et al, "Gamma-ray interactions with matter," *Passive Nondestructive Analysis of Nuclear Materials, Los Alamos National Laboratory*, pp. 27-42, 1991.

8 "Muons in tungsten (W)," [Online]. Available: http://pdg.lbl.gov/2014/AtomicNuclearProperties/MUE/muE_tungsten_W.pdf.

9 [Online]. Available: cosmic.lbl.gov.